Design and Implementation of the Space Vector Modulation for a Hexaphase Indirect Matrix Converter

Chabi Sanni, Augustin Mpanda Mabwe, Ahmed El Hajjaji

Design and Implementation of the Space Vector Modulation for a Hexaphase Indirect Matrix Converter

Chabi S. Sanni[1,3] Augustin Mpanda Mabwe[2] and Ahmed El Hajjaji[1]

[1]Laboratoire MIS, UPJV
33 rue Saint Leu, 80039 Amiens, France
E-Mail : salomon.sanni@unilasalle.fr, ahmed.hajjaji@u-picardie.fr
[2]SYMADE, UniLaSalle Amiens
14 Quai de la Somme, 80082 Amiens, France
E-Mail : augustin.mpanda@unilasalle.fr
[3]ADEME 20, avenue du Grésillé-
BP 90406 49004 Angers Cedex 01 France

ACKNOWLEDGMENT

This work was supported by the French Environment and Energy Management Agency (ADEME) and the Hauts de France Region.

***Index Terms*—PMSG, Matrix converter (MC), Indirect Matrix Converter (IMC), Space Vector Modulation (SVM), Voltage Transfer Ratio (VTR).**

***Abstract*—This work is a continuation of our research on high-performance (6-phase) permanent-magnet fault-tolerant synchronous generator (HPHSG). It focuses on interfacing the HPHSG source to the electrical distribution network via a matrix converter (MC) whose indirect topology (IMC) has six phases on the generator side and three phases on the grid side. In the literature, the most common MCs are three-phase and publication on multi-input converters with (N>3) are quite rare. The main objective of this paper is to develop a hexaphase IMC structure and its corresponding SVM control law. A closed-loop simulation of the system feeding a 1.35MW inductive load is carried out, and provides an overall evaluation of the system's performance.**

I. INTRODUCTION

Electricity generation from renewable energy sources has increased in recent years to reduce fossil fuel consumption and pollution levels. Wind power systems account for a significant amount of renewable energy. Variable-speed wind conversion systems have been developed in recent years, comprising a combination of generators and converters that are primarily managed by corresponding control systems. For the grid interfacing, the MC has garnered more interests, especially at the generation level as it replaces the classic back-to-back (B2B) converter while offering many advantages such as sinusoidal (input/output) currents, a unitary power factor besides being more compact and offering a longer life duration due to the absence of passive elements such as capacitors.

There are two types of MC, the conventional also called direct configuration (DMC) and the indirect configuration (IMC). Several publications on the indirect modulation technique of 3ϕ-to-3ϕ MC are available and refer to the Space Vector Modulation (SVM) whose maximum voltage transfer ratio (VTR) is 86%. So, it works as a step-down voltage [1] [2].

The multiphase machines (N>3) offer, among other intrinsic advantages, high power per unit , high fault tolerance, greater reliability, and low torque ripple rate. However, these machines require new converter structures to be interfaced to the grid. Several studies have been carried out on the improvement of the VTR and the overall efficiency of MCs.

In literature, more papers deal with the use of SVM on MCs applied to polyphase systems of type 3ϕ-to-Nϕ . The most studied systems are 3ϕ-to-5ϕ with 78.86% of VTR [3] [4], 3ϕ-to-7ϕ with 76.93% of VTR [5] and 3ϕ-to-9ϕ with a minimum VTR of 76% and maximum of 94.5% [6]. However, very few papers deal with Nϕ-to-3ϕ systems with MCs and their work are on DMC type. The papers [7] [8] develop SVM for a 5ϕ-to-3ϕ system applied to DMC using the direct SVM approach.

In a previous published paper [9], all possible config-

urations that can be generated from a 6ϕ-to-3ϕ IMC system were studied and presented with their corresponding VTRs. It shows three specific VTR values for the system of 50%, 78.9% and 96.6%.

In this paper, the system which is being studied is an IMC connected to the grid with 6ϕ-to-3ϕ hexaphase matrix converter as shown in Fig.1. The aim of this paper is to develop the indirect SVM modulation technique for all the rectifier and inverter stages and to evaluate the theorical part developped in [9].

To help understand the application presented in this paper, we firstly recall the modeling of the wind turbine and the PMSG, then the development of the SVM modulation technique for a 6ϕ-to-3ϕ IMC is described The SVM of the rectifier stage is based on the current space vectors of the 6 input phases while for the inverter stage the SVM is based on the voltage space vectors of the 3 output phases.

Finally, the whole system is modeled with the aim to define the VTR and to carry out an application case with an inductive load while using a LQR corrector for both control sides of the IMC in MATLAB/Simulink.

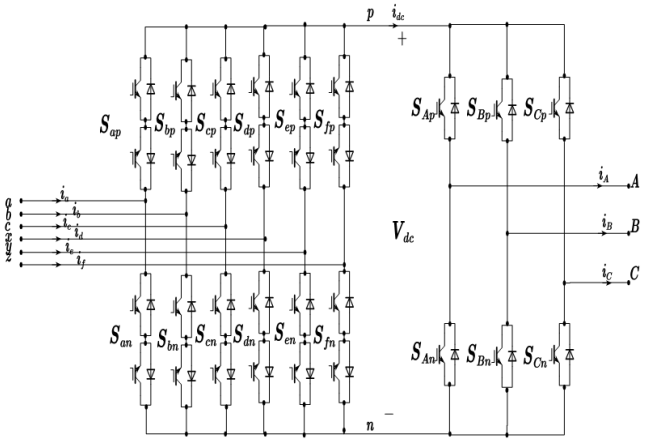

Fig. 1. Complete configuration of the hexaphase IMC.

II. System configuration

As depicted in the system overview scheme in Fig.2, the generator is coupled one side to the wind turbine directly without a gearbox and on the other side is connected to the IMC LC input filter. The IMC is interfaced to the grid through the LCL output filter. As it is classic for WECS, the MPPT control is used.

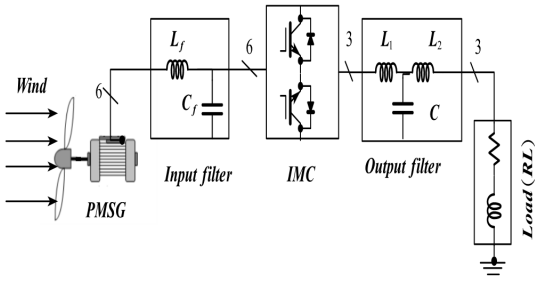

Fig. 2. System overview scheme without control.

III. WECS Modeling

A. Wind turbine model

The available mechanical power extracted from wind with a specific wind speed v_ω(m/s) is given by:

$$P_m = \frac{1}{2}(\rho)A_r v_\omega^3 C_p\left(\lambda,\beta\right) \quad (1)$$

The wind turbine mechanical torque output T_m given as :

$$T_m = \frac{P_m}{\omega_m} \quad (2)$$

where ρ is the air density (kg/m^3); A_r represents the swept area of the turbine blades (m^2); $C_p(\lambda,\beta)$ is the turbine power coefficient. The tip-speed ratio (λ represents the ratio between blade tip speed and wind speed) is defined as :

$$\lambda = \frac{\omega_m R}{v_\omega} \quad (3)$$

Where ω_m and R are the rotor angular velocity (in rad/sec) and rotor radius (in m), respectively. The power coefficient depends on the pitch angle of rotor blades β and of the tip speed ratio λ. $C_p(\lambda,\beta)$ is modeled using a standard equation that depends on the turbine characteristics [10]:

$$C_p(\lambda,\beta) = C_1((\frac{C_2}{\lambda_i}) - C_3\beta - C_4)e^{(-\frac{C_5}{\lambda_i})} + C_6\lambda \quad (4)$$

With $\frac{1}{\lambda_i} = ((\frac{1}{\lambda+0.08\beta}) - (\frac{0.035}{1+\beta^3}))$

$$C_1 = 0.5176; C_2 = 116; C_3 = 0.4; C_4 = 5;$$

$C_5 = 21$ *and* $C_6 = 0.0068$.

Fig.1 shows the characteristics of the wind turbine in which the relationship between C_p *and* λ from (4) is illustrated.

Thanks to Fig.3, we obtain the value of $C_{pmax} = 0.48$ and for $\beta = 0$ we obtained $\lambda_{opt} = 8.1$.

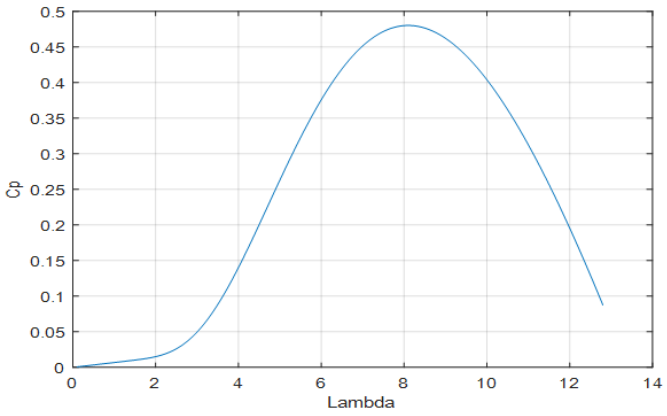

Fig. 3. $C_p(\lambda)$ characteristics.

B. PMSG Model

A nonlinear dynamic model of the six phase PSMG in the d-q transformed rotor reference frame is presented using the Vector Space Decomposition (VSD) approach. With VSD, the six-phase machine can be represented using three orthogonal subspaces, i.e., the d-q, x-y and the zero-sequence subspace.

$$\begin{cases} v_d = -L_d\left(\frac{di_d}{dt}\right) - R_s i_d + \omega_e L_q i_q \\ v_q = -L_q\left(\frac{di_q}{dt}\right) - R_s i_q - \omega_e(L_d i_d - \phi_m) \\ v_x = -L_0\left(\frac{di_x}{dt}\right) - R_s i_x \\ v_y = -L_0\left(\frac{di_y}{dt}\right) - R_s i_y \\ \frac{d}{dt}\omega_m = \frac{1}{J}(T_m - T_e - f\omega_m) \end{cases} \tag{5}$$

The electromagnetic torque of the PMSG is evaluated as :

$$T_e = 3p[(L_d - L_q)i_d i_q + i_q\phi_m)] \tag{6}$$

Where p is the number of pole pairs, L_d, L_q are the d-axis and q-axis stator inductance, L_0 is the stator self-leakage inductance. ϕ_m is the permanent magnet flux linkage and ω_m is the rotor angular speed.

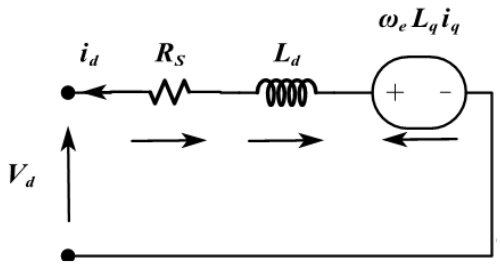

Fig. 4. d-axis equivalent circuit.

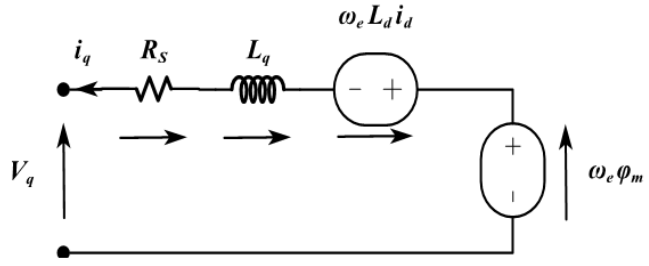

Fig. 5. q-axis equivalent circuit.

It is shown that the generator torque can be controlled through the stator q-axis current component only. For maximum output torque and high efficiency, the d, x and y-axis current are set to zero.

IV. Indirect Matrix Converter Model

The design of the indirect matrix converter (IMC) for the rectifier stage is based on twelve bidirectional switches, while the inverter stage is based on six single switches. Fig.6 provides a visual representation of the system's switches arrangement which is used in the space vector modulation (SVM) control.

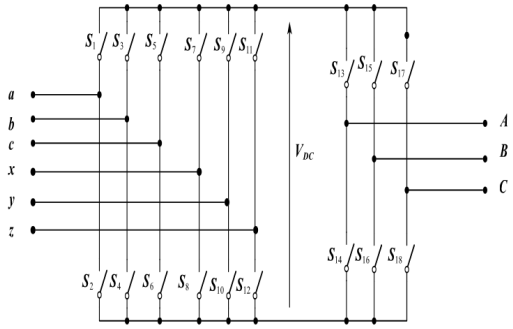

Fig. 6. Illustrative diagram of the hexaphase IMC.

The input voltage and current vectors expressions are as follows:

$$\begin{cases} V_{in} = (\frac{1}{3})\Big(V_a + V_b e^{j(\frac{2\pi}{3})} + V_c e^{j(\frac{4\pi}{3})} + \\ \qquad V_x e^{j(\frac{\pi}{6})} + V_y e^{j(\frac{5\pi}{6})} + V_z e^{j(\frac{3\pi}{2})}\Big) \\ I_{in} = (\frac{1}{3})\Big(I_a + I_b e^{j(\frac{2\pi}{3})} + I_c e^{j(\frac{4\pi}{3})} + \\ \qquad I_x e^{j(\frac{\pi}{6})} + I_y e^{j(\frac{5\pi}{6})} + I_z e^{j(\frac{3\pi}{2})}\Big) \end{cases} \tag{7}$$

The analytical expressions for the output voltage and current vectors are expressed according to (8) :

$$\begin{cases} V_{out} = (\frac{2}{3})\Big(V_A + V_B e^{j(\frac{2\pi}{3})} + V_C e^{j(\frac{4\pi}{3})}\Big) \\ I_{out} = (\frac{2}{3})\Big(I_A + I_B e^{j(\frac{2\pi}{3})} + I_C e^{j(\frac{4\pi}{3})}\Big) \end{cases} \tag{8}$$

The IMC stages are modeled as a matrix. The state vectors of the rectifier and inverter stages are given by (9) and (10).

For input vectors form, the variables controled are the input currents.

$$\begin{bmatrix} I_a \\ I_b \\ I_c \\ I_x \\ I_y \\ I_z \end{bmatrix} = \begin{bmatrix} S_1 & S_2 \\ S_3 & S_4 \\ S_5 & S_6 \\ S_7 & S_8 \\ S_9 & S_{10} \\ S_{11} & S_{12} \end{bmatrix} * \begin{bmatrix} I_{DC+} \\ I_{DC-} \end{bmatrix}$$

$$\begin{bmatrix} V_{DC+} \\ V_{DC-} \end{bmatrix} = \begin{bmatrix} S_1 & S_2 & S_3 & S_4 & S_5 & S_6 \\ S_7 & S_8 & S_9 & S_{10} & S_{11} & S_{12} \end{bmatrix} * \begin{bmatrix} V_a \\ V_b \\ V_c \\ V_x \\ V_y \\ V_z \end{bmatrix} \tag{9}$$

For output vectors form, the controled variables are the output voltages.

$$\begin{bmatrix} V_A \\ V_B \\ V_C \end{bmatrix} = \begin{bmatrix} S_{13} & S_{14} \\ S_{15} & S_{16} \\ S_{17} & S_{18} \end{bmatrix} * \begin{bmatrix} V_{DC+} \\ V_{DC-} \end{bmatrix}$$

$$\begin{bmatrix} I_{DC+} \\ I_{DC-} \end{bmatrix} = \begin{bmatrix} S_{13} & S_{15} & S_{17} \\ S_{14} & S_{16} & S_{18} \end{bmatrix} * \begin{bmatrix} I_A \\ I_B \\ I_C \end{bmatrix} \tag{10}$$

V. 6Φ-TO-3Φ IMC CONFIGURATIONS AND ASSOCIATED VTR

A. Active vectors of the inverter stage

The inverter stage is connected to an inductive load. By considering the interconnection laws of the energy sources, the output phases must not be open circuit. Then, the number of possible combinations of interconnections of phases is eight (2^3) with six active vectors and two zero vectors as shown in Table I. The complex plan is defined by the hexagon (Fig. 7).

TABLE I
INVERTER STAGE SWITCH COMBINATIONS

A	B	C	|Module|	Angle(rad)
0	0	0	0	–
0	0	1	$\frac{2}{3}V_{DC}$	$-\frac{2\pi}{3}$
0	1	0	$\frac{2}{3}V_{DC}$	$\frac{2\pi}{3}$
0	1	1	$\frac{2}{3}V_{DC}$	π
1	0	0	$\frac{2}{3}V_{DC}$	0
1	0	1	$\frac{2}{3}V_{DC}$	$-\frac{\pi}{3}$
1	1	0	$\frac{2}{3}V_{DC}$	$-\frac{\pi}{3}$
1	1	1	0	–

B. Active vectors of the rectifier stage

The rectifier stage is supplied by a voltage source. By considering the interconnection laws of the energy sources, the input phases must not be short-circuited. Then, the number of available combinations of interconnections of phases is thirty-six (6^2), thirty active vectors and six null vectors as shown in Table II and Table III with more details. Two complex plans are obtained and defined by Fig. 8 and Fig. 9.

TABLE II
RECTIFIER STAGE SWITCH COMBINATIONS

	a	**b**	**c**	**x**	**y**	**z**
a	–	ab	ac	ax	ay	az
b	ba	–	bc	bx	by	bz
c	ca	cb	–	cx	cy	cz
x	xa	xb	xc	–	xy	xz
y	ya	yb	yc	yx	–	yz
z	za	zb	zc	zx	zy	–

TABLE III
RECTIFIER STAGE SWITCH COMBINATIONS WITH DETAILS

	|Module|	Angle(°)		|Module|	Angle(°)
ab	0.5774	-30	xa	0.1725	105
ac	0.5774	30	xb	0.4714	-15
ad	0.1725	-75	xc	0.6440	45
ay	0.6440	-15	xy	0.5774	0
az	0.4714	45	xz	0.5774	60
ba	0.5774	150	ya	0.6440	165
bc	0.5774	90	yb	0.1725	-135
bx	0.4714	165	yc	0.4714	105
by	0.1725	45	yx	0.5774	180
bz	0.6440	105	yz	0.5774	120
ca	0.5774	-150	za	0.4714	-135
cb	0.5774	-90	zb	0.6440	-75
cx	0.6440	-135	zc	0.1725	-15
cy	0.4714	-75	zx	0.5774	-120
cz	0.1725	165	zy	0.5774	-60

C. Configurations and corresponding VTR

As discussed early in A and B, there are two complex plans for the rectifier stage and one complex plan for the inverter stage. They are used for the SVM control. For the rectifier plans, the first one is composed by the 18 active vectors and the second plan has 12 active vectors.

As the MC is a step-down converter, it is important to determine the maximum VTR that the system can achieve using the complex plans of the rectifier stage and the inverter stage.

with the 3 complex plans, 3 configurations are defined for the SVM control development.

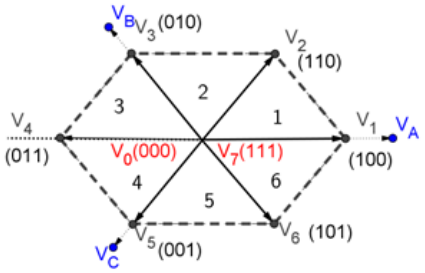

Fig. 7. Complex plan of the inverter stage.

$Do_{vectors}$ (Scheme1): Use of the 12 active vectors of the Dodecagon for the control with the magnitude of |D|=0.5774V_{DC}.

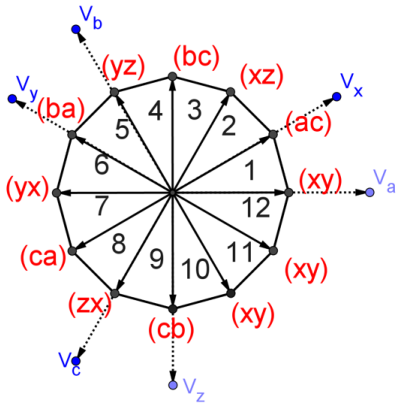

Fig. 8. VSR Dodecagon active vectors complex plan.

The hexagon with 18 active vectors (Fig. 9) leads to 3 main groups of active vector amplitudes which are: Large: |L|=0.6440Vdc, Medium: |M|=0.4714V_{DC} and Small: |S|=0.1725V_{DC}.

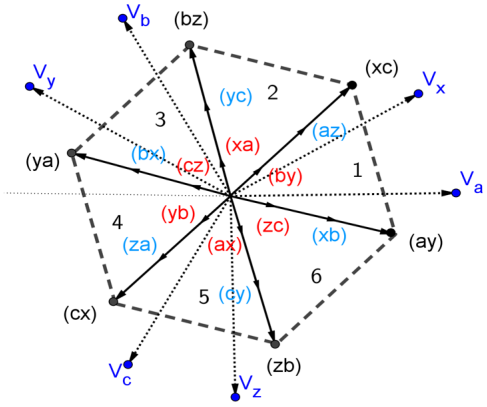

Fig. 9. VSR 18 active vectors complex plan.

$Sx_{vectors}$ (Scheme2): Use of the six large active vectors

$Tw_{vectors}$ (Scheme3): Use of the six large and six medium actives vectors

Table IV summarises the VTR for the three configurations.

TABLE IV
CONSIDERED CONFIGURATIONS AND VTR

Configurations	m_c	m_v	**VTR (%)**
3ϕ-to- 3ϕ	$\frac{I_{ref}}{I_d}$	$\sqrt{3}\frac{V_{ref}}{V_d}$	86.6
(6ϕ-to- 3ϕ) Scheme1	$3.464\frac{I_{ref}}{I_d}$		50
(6ϕ-to- 3ϕ) Scheme2	$1.793\frac{I_{ref}}{I_d}$		96.6
(6ϕ-to- 3ϕ) Scheme3	$m_c = 2.196\frac{I_{ref}}{I_d}$		78.9
	$m'_c = 2.45\frac{I_{ref}}{I_d}$		
	$m''_c = 1.793\frac{I_{ref}}{I_d}$		

Based on the results of Table IV, the $Sx_{vectors}$ (Scheme2) and $Tw_{vectors}$ (Scheme3) configurations are choosen and their SVM controls are developped.

VI. SVM SETUP OF INDIVIDUAL STAGE

For the SVM setup, all input reference signals, six currents for the VSR stage and three voltages for the VSI, are transformed to $\alpha\beta$ reference frame. The SVM setup for the inverter stage is the same for both scheme2 and scheme3, but for the rectifier stage the SVM setup is different for each configuration.

A. Inverter stage

Fig. 7 has 6 sectors, the projections of the sector voltage reference vector V^* onto the α and β axes are V_α and V_β.

The duty cycles expressions of the vectors V_α and V_β in each sector are calculated as follows :

$$\begin{cases} d_\alpha = \frac{T_\alpha}{T_s} = m_v.\sin\left(\frac{\pi}{3} - \theta_v\right) \\ d_\beta = \frac{T_\beta}{T_s} = m_v.\sin\left(\theta_v\right) \\ d_{ov} = \frac{T_{ov}}{T_s} = 1 - d_\alpha - d_\beta \\ V^* = V_\alpha d_\alpha + V_\beta d_\beta + V_{ov} d_{ov} \end{cases} \quad (11)$$

With m_v being the inverter modulation index, 0$\leq$ m_v $\geq$1 and θ_v is the angle in each sector, 0<θ_v>60°.

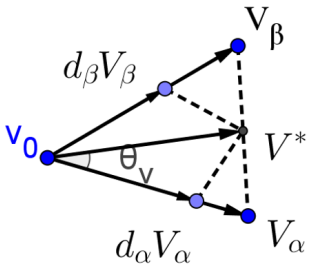

Fig. 10. VSI SVM vector sector.

To minimize the number of commutations per switch, the vector switching sequence used, called double-sided switching sequence [3], is given as:

$$\overrightarrow{V_\alpha} \Rightarrow \overrightarrow{V_\beta} \Rightarrow \overrightarrow{V_{ov}} \Rightarrow \overrightarrow{V_\beta} \Rightarrow \overrightarrow{V_\alpha} \tag{12}$$

B. Rectifier stage (Scheme2)

From the complex plan of Fig.9 and considering the chosen configuration, only the six active vectors with the highest amplitudes should be used as shown by the complex plan defined by the hexagon below (Fig. 11).

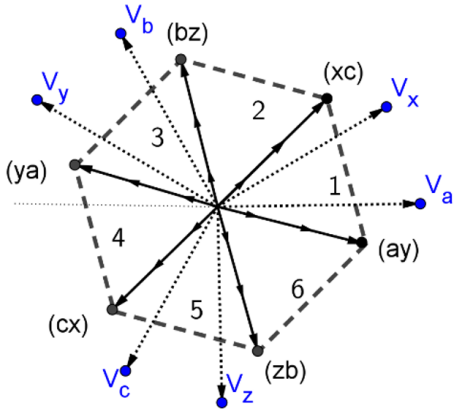

Fig. 11. VSR 6 active vectors (Scheme2) complex plan.

The projections of the sector reference current vector I^* on the γ and δ axes are designed by I_γ and I_δ.

The corresponding duty cycles expressions are then:

$$\begin{cases} d_\gamma = \frac{T_\gamma}{T_s} = m_c.\sin\left(\frac{\pi}{3} - \theta_c\right) \\ d_\delta = \frac{T_\delta}{T_s} = m_c.\sin\left(\theta_c\right) \\ d_{oc} = \frac{T_{oc}}{T_s} = 1 - d_\gamma - d_\delta \\ I^* = I_\gamma d_\gamma + I_\delta d_\delta + I_{oc} d_{oc} \end{cases} \tag{13}$$

With m_c being the rectifier modulation index. Usually, it is set to 1 to keep the DC bus current equal to the input current. θ_c is the angle in each sector, $0<\theta_c>60°$.

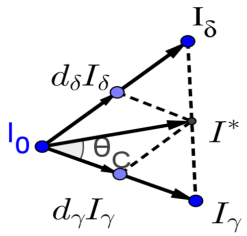

Fig. 12. VSR SVM vector sector Scheme2.

According to the double-sided switching sequence, it comes as (14):

$$\overrightarrow{I_\gamma} \Rightarrow \overrightarrow{I_\delta} \Rightarrow \overrightarrow{I_{oc}} \Rightarrow \overrightarrow{I_\delta} \Rightarrow \overrightarrow{I_\gamma} \tag{14}$$

C. Rectifier stage (Scheme3)

From the complex plan of Fig.9, and considering the chosen configuration, the six large and six medium active vectors are used as shown by the complex plan defined by the hexagon below (Fig. 13).

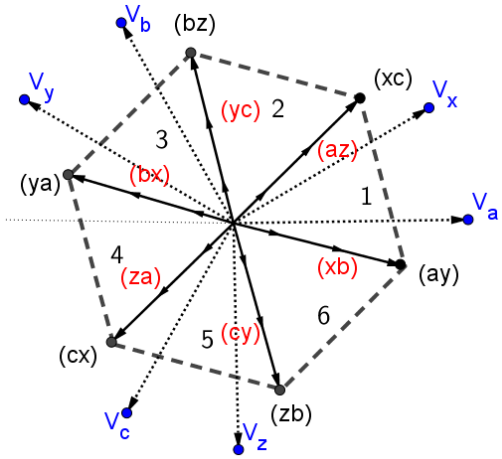

Fig. 13. VSR 12 active vectors (Scheme3) complex plan.

Fig.13 shows that in each sector there are 4 vectors. Their projections on the γ and δ axes lead to 4 components, two on each axes, for the sector reference current vector I^* . Those components are I'_γ, I'_δ, I''_γ and I''_δ as according to Fig.14.

The duty cycles expressions are deduced as:

$$\begin{cases} d'_\gamma = \frac{T'_\gamma}{T_s} = m'_c.\sin\left(\frac{\pi}{3} - \theta_c\right) \\ d''_\gamma = \frac{T''_\gamma}{T_s} = m''_c.\sin\left(\frac{\pi}{3} - \theta_c\right) \\ d'_\delta = \frac{T'_\delta}{T_s} = m'_c.\sin\left(\theta_c\right) \\ d''_\delta = \frac{T''_\delta}{T_s} = m''_c.\sin\left(\theta_c\right) \\ d_{oc} = \frac{T_{oc}}{T_s} = 1 - d'_\gamma - d'_\delta - d''_\gamma - d''_\delta \\ \\ I^* = I'_\gamma d'_\gamma + I''_\delta d''_\delta + I''_\gamma d''_\gamma + I'_\delta d'_\delta + I_{oc} d_{oc} \end{cases} \tag{15}$$

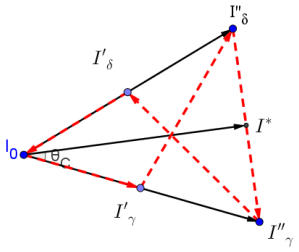

Fig. 14. VSR SVM vector sector Scheme3.

With m'_c and m''_c the rectifier modulation index for medium and large vectors respectively. Usually, it is set to 1 to keep the DC bus current equal to the input current. θ_c is the angle in each sector, $0<\theta_c>60°$.

According to the double-sided switching sequence, it is as follows:

$$\overrightarrow{I'_\gamma} \Rightarrow \overrightarrow{I''_\delta} \Rightarrow \overrightarrow{I''_\gamma} \Rightarrow \overrightarrow{I'_\delta} \Rightarrow \overrightarrow{I_{oc}} \Rightarrow \overrightarrow{I'_\delta} \Rightarrow \overrightarrow{I''_\gamma} \Rightarrow \overrightarrow{I''_\delta} \Rightarrow \overrightarrow{I'_\gamma} \quad (16)$$

VII. Synchronization of the two stages for the complete system

As the MC has no capacitor for system stabilization, the control strategies of the two stages must be synchronized to ensure proper converter operation. The rectifier stage (for each configuration) and the inverter stage are combined for synchronized control.

A. Scheme2 Configuration

The duty cycles of the complete system for this configuration are as follows:

$$\begin{cases} d_{\alpha\gamma} = \frac{T_{\alpha\gamma}}{T_s} = m.\sin(\frac{\pi}{3}-\theta_v)sin(\frac{\pi}{3}-\theta_c) \\ d_{\alpha\delta} = \frac{T_{\alpha\delta}}{T_s} = m.\sin(\frac{\pi}{3}-\theta_v)sin(\theta_c) \\ d_{\beta\gamma} = \frac{T_{\beta\gamma}}{T_s} = m.\sin(\theta_v)sin(\frac{\pi}{3}-\theta_c) \\ d_{\beta\delta} = \frac{T_{\beta\delta}}{T_s} = m.\sin(\theta_v)sin(\theta_c) \end{cases} \quad (17)$$

With m=$m_c.m_v$.
For the simplification of the control, the zero vectors of the currents are neglected and only the zero vectors of the voltages are used. During the remaining part of the switching period T_s, the zero vector is applied:

$$d_o = \frac{T_o}{T_s} = 1 - d_{\alpha\gamma} - d_{\alpha\delta} - d_{\beta\gamma} - d_{\beta\delta} \quad (18)$$

B. Scheme3 Configuration

Their are eight duty cycles for the complete system of this configuration. Four for the medium vectors and four for the large vectors. Below are the duty cycles for the medium vectors:

$$\begin{cases} d'_{\alpha\gamma} = \frac{T'_{\alpha\gamma}}{T_s} = m'.\sin(\frac{\pi}{3}-\theta_v)sin(\frac{\pi}{3}-\theta_c) \\ d'_{\alpha\delta} = \frac{T'_{\alpha\delta}}{T_s} = m'.\sin(\frac{\pi}{3}-\theta_v)sin(\theta_c) \\ d'_{\beta\gamma} = \frac{T'_{\beta\gamma}}{T_s} = m'.\sin(\theta_v)sin(\frac{\pi}{3}-\theta_c) \\ d'_{\beta\delta} = \frac{T'_{\beta\delta}}{T_s} = m'.\sin(\theta_v)sin(\theta_c) \end{cases} \quad (19)$$

With m'=$m'_c.m_v$ the medium vectors modulation index.
The duty cycles for the large vectors are as for medium vectors with the modulation index m''=$m''_c.m_v$.
As previously, the zero vectors of the currents are neglected. During the remaining part of the switching period T_s, the zero vector is applied:

$$d_o = \frac{T_o}{T_s} = 1-d'_{\alpha\gamma}-d'_{\alpha\delta}-d'_{\beta\gamma}-d'_{\beta\delta}-d''_{\alpha\gamma}-d''_{\alpha\delta}-d''_{\beta\gamma}-d''_{\beta\delta} \quad (20)$$

C. Zero vector choice

The aim of this step is to choose a zero vector that can be either [000] or [111] and not both at the same time, in order to obtain the smallest possible switching sequence. Possible zero vectors are [aaa], [bbb], [ccc], [xxx], [yyy] or [zzz].

VIII. Switching strategy for switches control

Once the stages have been synchronized and the zero vector chosen, the overall switching sequence of the stages can be implement.

A. Standard strategy

The standard strategy is implemented using the doubled-sided switching sequence previously explained for both stage and it comes as follows:

- Scheme2

$$\alpha\gamma - \beta\gamma - \beta\delta - \alpha\delta - \overrightarrow{0} - \alpha\delta - \beta\delta - \beta\gamma - \alpha\gamma \quad (21)$$

Example: The signals are in sector 1 of current and sector 1 of voltage, the double-sided switching sequence is then deduced as:

$$\overrightarrow{I_1V_1} \rightarrow \overrightarrow{I_1V_2} \rightarrow \overrightarrow{I_2V_2} \rightarrow \overrightarrow{I_2V_1} \rightarrow \overrightarrow{0} \rightarrow \overrightarrow{I_2V_1} \rightarrow \overrightarrow{I_2V_2} \rightarrow \overrightarrow{I_1V_2} \rightarrow \overrightarrow{I_1V_1} \quad (22)$$

- Scheme3

$$\alpha\gamma' - \beta\gamma' - \beta\delta'' - \alpha\delta'' - \alpha\gamma'' - \beta\gamma'' - \beta\delta' - \alpha\delta' - \overrightarrow{0} - \ldots \quad (23)$$

Please note that the other side of the equation (23) mirrors the first part as for Scheme2.

Example: The signals are in sector 1 of current and sector 1 of voltage, the double-sided switching sequence is expressed as:

$$\overrightarrow{I_1V_1} \rightarrow \overrightarrow{I_1V_2} \rightarrow \overrightarrow{I_4V_2} \rightarrow \overrightarrow{I_4V_1} \rightarrow \overrightarrow{I_2V_1} \rightarrow \overrightarrow{I_2V_2} \rightarrow \overrightarrow{I_3V_2} \rightarrow \overrightarrow{I_3V_1} \rightarrow \overrightarrow{0} \rightarrow \ldots (24)$$

B. Optimized strategy

The aim of the strategy is to minimize the number of switchings or Branch-Switch-Over (BSO) of the entire matrix converter. For a number vector sequence, nine for Scheme2 and eighteen for Scheme3, there is a minimum number of BSO at which the sequence can be realized. This is unfortunately not always the case and the number of BSO is more than the minimum.

An optimized strategy developed in [2] offers the possibility to minimize in each sequence the number of BSO.

This stategy consists of changing the direction of the sequence of the voltage vectors at the level of the sectors when the number of BSO obtained exceeds the minimum. The corresponding switching order is then as:

- Scheme2

$$\beta\gamma - \alpha\gamma - \alpha\delta - \beta\delta - \overrightarrow{0} - \beta\delta - \alpha\delta - \alpha\gamma - \beta\gamma \quad (25)$$

- Scheme3

$$\beta\gamma' - \alpha\gamma' - \alpha\delta'' - \beta\delta'' - \beta\gamma'' - \alpha\gamma'' - \alpha\delta' - \beta\delta' - \overrightarrow{0} - \ldots \quad (26)$$

Again, please note that the other side of the equation (26) mirrors the first part as for Scheme2.

The whole procedure for each configuration is summarized in Table V and VI.

TABLE V
SWITCHING SEQUENCES FOR $Sx_{vectors}$ (SCHEME2)

Switching sequence: standard strategy					
Rectifier stage switching	S_γ		S_δ		
Inverter stage switching	S_α	S_β	S_β	S_α	S_0
Synchronized duty cycle	$\frac{1}{2}d_\gamma d_\alpha$	$\frac{1}{2}d_\gamma d_\beta$	$\frac{1}{2}d_\delta d_\beta$	$\frac{1}{2}d_\delta d_\alpha$	$\frac{1}{2}d_0$
	$\frac{T_s}{2}$				

- Zero vector

$$S_0 = \begin{cases} 111, & if\ K_v\ is\ even \\ 000, & if\ K_v\ is\ odd \end{cases} \quad (27)$$

With K_v the number of voltage sectors at a given time.

TABLE VI
SWITCHING SEQUENCES FOR $Tw_{vectors}$ (SCHEME3)

If $K = K_I + K_V$ is odd (Switching sequence: optimized strategy)									
Rectifier stage switching	S'_γ		S''_δ		S''_γ		S'_δ		S_0
Inverter stage switching	S_β	S_α	S_α	S_β	S_β	S_α	S_α	S_β	
Synchronized duty cycle	$\frac{1}{2}d'_\gamma d_\beta$	$\frac{1}{2}d'_\gamma d_\alpha$	$\frac{1}{2}d''_\delta d_\alpha$	$\frac{1}{2}d''_\delta d_\beta$	$\frac{1}{2}d''_\gamma d_\beta$	$\frac{1}{2}d''_\gamma d_\alpha$	$\frac{1}{2}d'_\delta d_\alpha$	$\frac{1}{2}d'_\delta d_\beta$	$\frac{1}{2}d_0$
If $K = K_I + K_V$ is even (Switching sequence: standard strategy)									
Rectifier stage switching	S'_γ		S''_δ		S''_γ		S'_δ		S_0
Inverter stage switching	S_α	S_β	S_β	S_α	S_α	S_β	S_β	S_α	
Synchronized duty cycle	$\frac{1}{2}d'_\gamma d_\alpha$	$\frac{1}{2}d'_\gamma d_\beta$	$\frac{1}{2}d''_\delta d_\beta$	$\frac{1}{2}d''_\delta d_\alpha$	$\frac{1}{2}d''_\gamma d_\alpha$	$\frac{1}{2}d''_\gamma d_\beta$	$\frac{1}{2}d'_\delta d_\beta$	$\frac{1}{2}d'_\delta d_\alpha$	$\frac{1}{2}d_0$
	$T_s/2$								

- Zero vector

$$S_0 = \begin{cases} 111, & if\ K_I\ is\ even \\ 000, & if\ K_I\ is\ odd \end{cases} \quad (28)$$

With $K_I, K_V\ and\ K$ respectively representing the current and voltage sectors and the sum of the values of these two sectors at a given time.

IX. SIMULATION RESULTS

The WECS, the IMC are modeled and their SVM control is implemented in detail in MATLAB/Simulink as shown in Fig. 2. The generator is controled by an MPPT controller to extract the maximum power from the available wind. The switches of the IMC are controled by the SVM command adapted to the topology of Fig. 1. The output control strategy used is direct voltage control

(stand-alone mode). An input filter and an output filter are added to the system. LQR controllers are used for dq signal correction in closed loop to control the rectifier stage but the inverter stage is in open loop to verify whether the theoretical VTR is obtained.

TABLE VII
SIMULATION PARAMETERS

PMSG	S_n=1.5MVA, Pôles=80, R_s=3.17 mΩ, $L_d = L_q$=3.07 mH, J=10000 kg.m^2, ϕ_m=7.0172 Wb, f=0	
Turbine	Radius=35.25 m, ρ=1.225 $\frac{kg}{m^3}$, V_w=11m/s	
Input filter	$L_f = 0.534mH$	$C_f = 0.0053F$
Load	$R_c = 0.463\Omega$, $L_c = 713.37\mu$H	
Output filter	$L_1 = 6.1mH, L_2 = 0.165mH$	$C = 278\mu$F

Fig.15 to Fig.17 illustrate the input current and output voltage for a 3ϕ-to-3ϕ system and for the two 6ϕ-to-3ϕ system configurations.

On Fig.15 the voltage and current waveforms and the THDs obtained for the 3ϕ-to-3ϕ system are $< 5\%$, which is reasonable (see Table VIII).

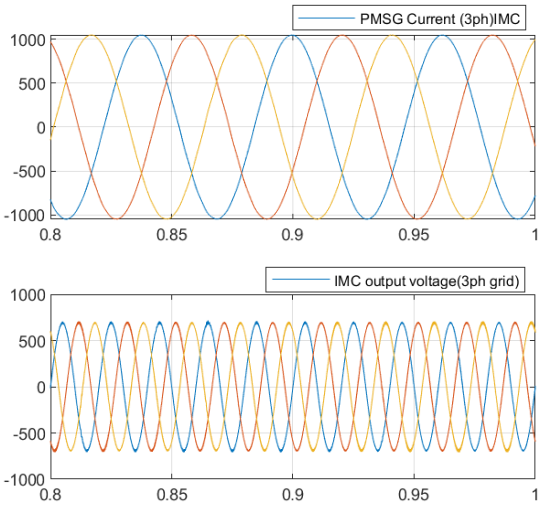

Fig. 15. PMSG currents and load voltages for 3ϕ-to-3ϕ system.

On Fig.16 the input current of the 6ϕ-to-3ϕ (Scheme2) system shows phase jumps at various levels, certainly due to the use of 6 active vectors out of a total of 30. As a result, the THD is $> 5\%$, with the presence of rank 3 harmonics.

On Fig.17 the input current of the 6ϕ-to-3ϕ (Scheme3) has a better signal and the THD is lower than scheme2 configuration, Table VIII shows those datas.

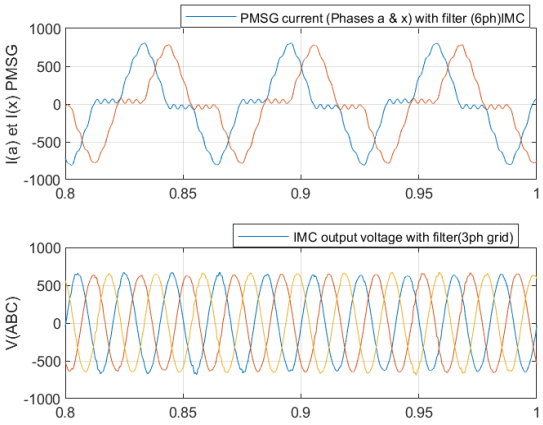

Fig. 16. PMSG currents and load voltages for $Sx_{vectors}$ (Scheme2) 6ϕ-to-3ϕ system.

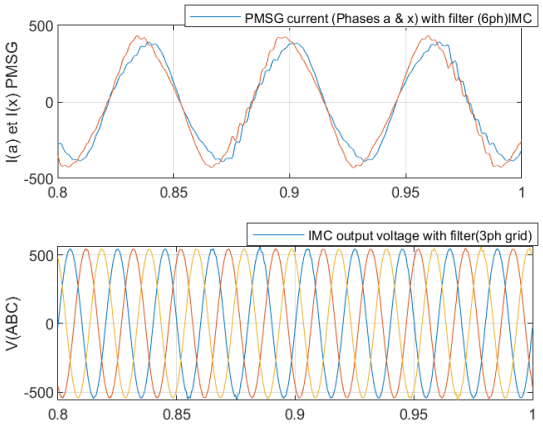

Fig. 17. PMSG currents and load voltages for $Tw_{vectors}$ (Scheme3) 6ϕ-to-3ϕ system.

By analyzing the signals on Fig.16 to Fig.17, it becomes clear that more active vectors are used in the rectifier stage, the waveform is more perfect and a low THD is obtained, but at the loss of VTR ratio.

Table VIII contains the magnitudes and THD of signals of each configuration system. It is worth noting that the current obtained at the IMC output is quite high due to the power of the generator. In a physical system, it would be necessary to adapt the wind speed for a lower power or to insert a step-up transformer between the CMI and the load, which would reduce the value of the current.

X. CONCLUSION

The complete mathematical model of the system under study is deployed in the MATLAB/Simulink environment. The various possible SVM configurations applied to the hexaphase system are then studied. A detailed explanation of the implementation of space

vector modulation (SVM) was provided, and simulations were carried out for the configurations scheme2 with VTR 96.6% and scheme3 with VTR 78.9%. This study shows that with a lower number of phases, Nϕ-to-3ϕ IMC systems give a higher VTR than a 3ϕ-to-Nϕ IMC systems (e.g. 6ϕ-to-3ϕ VTR_{max}= 96.6% and 3ϕ-to-9ϕ VTR_{max} =94.5%).

The closed-loop simulation of the system feeding a 1.35MW inductive load is performed in the Matlab/Simulink environment. The results show that the VTRs obtained are very close to the theoretical ones. Looking ahead, we will implement closed loop control for a load-supply system connected to the grid, and carry out the experimental part.

TABLE VIII
SIMULATION RESULTS FOR ALL CONFIGURATIONS

	3ϕ−to−3ϕ		**6ϕ − to−3ϕ** $Sx_{vectors}$ **(Scheme2)**		**6ϕ−to−3ϕ** $Tw_{vectors}$ **(Scheme3)**	
	Max values	THD (%)	Max values	THD (%)	Max values	THD (%)
V_{PMSG} (V)	834.7	0.02	742.3	0.09	742.3	0.09
I_{PMSG} (A)	1049	0.29	558.6	41.59	404.8	7.79
$V_{in\,MC}$ (V)	832.1	1.13	733.2	6.45	738.3	2.26
$I_{in\,MC}$ (A)	1041	64	545.4	106.7	388.4	138
$V_{out\,MC}$ (V)	719.8	75.55	691.3	80.10	565.9	87.32
V_{load} (V)	687.7	1.11	645.1	2.12	540.2	0.65
I_{load} (A)	1337	0.07	1254	0.92	1050	0.11
VTR (%)	86.5		95.4		76.6	

REFERENCES

[1] L. Huber et D. Borojevic, “Space vector modulated three-phase to three-phase matrix converter with input power factor correction”, IEEE Trans. Ind. Appl., vol. 31, no 6, p. 1234-1246, déc. 1995, doi: 10.1109/28.475693.

[2] P. Nielsen, F. Blaabjerg, et J. K. Pedersen, “Space vector modulated matrix converter with minimized number of switchings and a feedforward compensation of input voltage unbalance”, in Proceedings of International Conference on Power Electronics, Drives and Energy Systems for Industrial Growth, New Delhi, India: IEEE, 1995, p. 833-839. doi: 10.1109/PEDES.1996.536381.

[3] M. Chai, R. Dutta, et J. Fletcher, “Space vector PWM for three-to-five phase indirect matrix converters with d2-q2 vector elimination”, in IECON 2013 - 39th Annual Conference of the IEEE Industrial Electronics Society, Vienna, Austria: IEEE, nov. 2013, p. 4937-4942. doi: 10.1109/IECON.2013.6699934.

[4] Q.-H. Tran et H.-H. Lee, “An Advanced Modulation Strategy for Three-to-Five-Phase Indirect Matrix Converters to Reduce Common-Mode Voltage With Enhanced Output Performance”, IEEE Trans. Ind. Electron., vol. 65, no 7, p. 5282-5291, juill. 2018, doi: 10.1109/TIE.2017.2782242.

[5] S. M. Ahmed, Z. Salam, et H. Abu-Rub, “Improved Space Vector Modulation for Three-to-Seven Phase Matrix Converter with Reduced Number of Switching Vectors”, IEEE Trans. Ind. Electron., p. 1-1, 2014, doi: 10.1109/TIE.2014.2381158.

[6] S. M. Dabour, S. M. Allam, et E. M. Rashad, “Indirect space-vector PWM technique for three to nine phase matrix converters”, in 2015 IEEE 8th GCC Conference Exhibition, Muscat, Oman: IEEE, févr. 2015, p. 1-6. doi: 10.1109/IEEEGCC.2015.7060029.

[7] S. M. Ahmed, H. Abu-Rub, Z. Salam, et A. Iqbal, “Space vector PWM technique for a direct five-to-three-phase matrix converter”, in IECON 2013 - 39th Annual Conference of the IEEE Industrial Electronics Society, Vienna, Austria: IEEE, nov. 2013, p. 4943-4948. doi: 10.1109/IECON.2013.6699935.

[8] M. Mihret, M. Abreham, O. Ojo, et S. Karugaba, “Modulation schemes for five-phase to three-phase AC-AC matrix converters”, in 2010 IEEE Energy Conversion Congress and Exposition, Atlanta, GA: IEEE, sept. 2010, p. 1887-1893. doi: 10.1109/ECCE.2010.5618296.

[9] C. S. Sanni, A. Mpanda Mabwe, et A. El Hajjaji, “Power Quality Analysis of Six Phase Indirect Matrix Converter Based on Multi Phase Generator”. Renewable Energy and Power Quality Journal, vol. 21, no 1, juillet 2023, p. 575-82. DOI.org (Crossref), https://doi.org/10.24084/repqj21.403.

[10] S. K. Bisoyi, “Modeling and Analysis of Variable Speed Wind Turbine equipped with PMSG”, Int. J. Curr. Eng. Technol., vol. 2, no 2, p. 421-426, janv. 2013, doi: 10.14741/ijcet/spl.2.2014.78.